



Effects of Vibration on Microstructure and Thermal Properties of Friction Stir Spot Welded (FSSW) Aluminum Alloy (Al5083)

Behrouz Bagheri¹ · Mahmoud Abbasi² · Mohammad Givi²

Received: 19 November 2018 / Revised: 8 April 2019 / Accepted: 21 April 2019 / Published online: 22 May 2019
© Korean Society for Precision Engineering 2019

Abstract

Friction stir spot welding (FSSW) is a solid state joining technique with a simple concept. A non-consumable rotating tool with a specially designed pin and shoulder are inserted into the sheets or plates to be joined. In this study, the effect of vibration on microstructure and thermal properties of Al5083 weldment made by FSSW using rotation speed of 1500 rpm and different dwelling times, namely 5 and 10 s, was investigated. This new method was entitled FSSVW (friction-stir-spot-vibration welding). The experimental and numerical results, obtained using Abaqus software, were compared. In this work, the Johnson–Cook hardening condition was used for modeling of deformable metals. The results showed good comparability between experimental and FEM data. Also, metallography analyses indicated that the grain size decreased and the temperature increased as FSSVW method was applied. The results showed that vibration during FSSW leads to grain size decrease of about 30–50% in the weld region.

Keywords Friction stir spot welding · Johnson–Cook hardening · Mechanical properties · Finite element analysis

List of Symbols

FSSW	Friction stir spot welding
FSSVW	Friction stir spot vibration welding
S-FSSVW	Simulation of friction stir spot vibration welding
ALE	Arbitrary Lagrangian–Eulerian
JCP	Johnson–Cook Plasticity
EDS	Energy dispersive spectrometry
σ	Static yield stress (MPa)
ε	Equivalent plastic strain (%)
HAZ	Heat-affected zone
TMAZ	Thermo-mechanical affected zone
WNZ	Weld nugget zone
SZ	Stir zone
Z	Zener–Hollomon parameter
R	Gas constant
SEM	Scanning electron microscopy
ω	Rotation speed (rpm)
v	Traverse speed (mm/min)

1 Introduction

In the past decades, the welding technique has applied to a wide range of materials in industrial applications. Friction stir spot welding (FSSW) is a solid-state joining process where a non-consumable rotating tool inserted into the work-piece, and the friction created between tool and work-piece generates heat, and the material adjacent to the tool is softened. The localized region of softened material moved around the tool under a plastic flow resulting in a solid-phase bond between the materials to be welded. FSSW is considerable interest in joining many metals such as magnesium, titanium, copper, and their alloys, and also enables joining of polymers, dissimilar materials and, composite [1–8]. Friction stir spot welding (FSSW) is a spot variant of FSW applied to a lap joint consisting of an upper and lower plate, and there are several versions of FSSW, but the simple method was used in this research (Fig. 1).

There are many parameters to vary in FSSW namely rotation speed, dwell time, plunge rate, cooling of work-piece, preheating, flow materials, post heat treatment, and etc. [9–15]. Tuncel et al. [16] investigated the mechanical properties of AA6082 joints by FSSW. The results showed that the tensile shear load increased with increasing plunge depth and dwell time, and the tensile shear load decreased linearly by increasing rotational speed and feed rate. Abhijit Dey et al.

✉ Behrouz Bagheri
b.bagheri@aut.ac.ir

¹ Department of Mining and Metallurgy, Amirkabir University of Technology, Tehran, Iran

² Faculty of Engineering, University of Kashan, Kashan, Iran

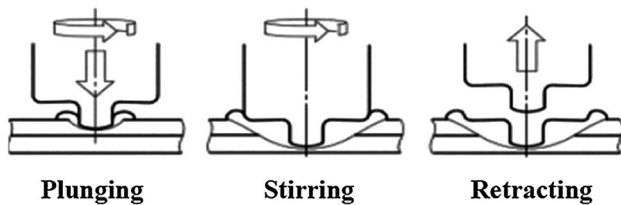


Fig. 1 Schematic illustration of FSSW [8]

[17] determined the mechanical properties of aluminum alloys joints made by FSSW. They found that the welding process softened the material and reduced the hardness to 33% of the parent material. Microstructure and mechanical properties of FSS-welded for galvanized steel was investigated by Baek et al. [18]. The results indicated that the increasing tool penetration depth led to enhancement of the tensile shear strength to a maximum value of 3.07 kN at a tool penetration depth of 0.52 mm and also ZnO was observed in the deformation region during FSSW. Sheikhasani et al. [19] studied the effect of FSSW parameters on mechanical properties of the joint developed between galvanized steel plates. They indicated that the grain size decreased by 23% in SZ and 15% in TMAZ with increasing shoulder diameter from 10 to 14 mm. The mechanical properties, namely tensile shear strength, of EN AW 5005 joint made by FSSW were investigated by Kulecki [20]. He found that the weld performance is dependent on the tool rotation, dwell time, and the tool pin height and also there is an optimum tool pin height to obtain the highest tensile shear strength.

In FSSW, the maximum temperature of the welded plates typically ranges from 70 to 90% of the melting temperature of the work-piece material [21]. Khunder et al. [22] studied the numerical simulation of the temperature distribution of AA2014 joints during FSSW. The FEM results had good agreement with those recorded experimentally and the peak temperature obtained was 50% of the melting point of the base material. Thermo-mechanical characteristics of FSS-welded HDPE plates determined by Quazi et al. [23]. They reported the optimum value of lap shear strength at 4.01 kN for intermediate values of welding parameter such as 980 rpm, 12.5 mm/min, the 60 s and 6.8 mm for rotational tool speed, the plunge rate, dwell time and pin depth, respectively. Numerical simulation of FSSW was applied to lap shear test of magnesium alloys by Campanelli et al. [24]. In their study, they concentrated the plastic flow in the vicinity of the welded zone where tensile stresses reached the highest values, inducing permanent damage.

In this study, the complete process of FSSW in Al5083 joining in rotational speed of 1500 rpm and two dwelling time (5 and 10 s) was simulated using finite element method (FEM) by application of Abaqus software. The predictions had verified by experimental results. Additionally,

a modified version of FSSW, entitled FSSVW, was introduced. Microstructure characteristics of weld developed by the modified welding process were compared with those of weld resulted from conventional FSSW process.

2 Experimental and Method

2.1 Materials

AA5083 aluminum alloy sheets with thicknesses of 2 mm and 0.7 mm were used as joining materials. Sheets were cut into pieces in dimensions of 100 mm length and 25 mm width, and these pieces were FSS-welded in the overlapping configuration. Figure 2 shows the Energy dispersive spectrometry (EDS) curves AA5083 alloy. The chemical composition of the base material was specified by Spark Emission Spectrometer, and the mechanical properties were tested by the stress–strain test. These results are presented in Tables 1 and 2, respectively.

According to Fig. 3a, the vibration was applied through the fixture. Rotation movement of the motor shaft was transformed to linear motion of fixture using a camshaft. The motor was equipped by a driver to bring the possibility to change the motor rotation speed. The tool has consisted of a circular shoulder and a trapezoidal pin. The pin was made of tungsten carbide, and the shoulder was prepared from M2 steel (Fig. 3b). To find the effect of the developed welding method on microstructure and mechanical properties different welding conditions were applied. These conditions are presented in Table 3. For each situation, both welding processes, FSSW and FSSVW, were done.

Metallography samples were prepared from the cross sections of the welded specimens, and they were subjected to grinding, polishing, and etching with an etchant solution consisted of 12 ml HNO₃, 15 ml HF, 128 ml H₂O, and 45 ml HCL for about 20–30 s.

The grain size was evaluated by optical microscopy, and it was measured through the mean linear intercept method [25]. Firstly, a square of the selected area (300 × 300 μm²) overlaid on a micrograph and the numbers of grains including the grains entirely within the known area plus one half of the number of grains intersected by the circumference of the region were counted. Finally, the number of grains per unit area was calculated and then, the average diameter of the grains was estimated assuming the grains to be spherical.

2.2 Numerical Simulation

To capture severe deformation during the FSSW process an arbitrary Lagrangian–Eulerian (ALE) formulation was adopted in Abaqus/Explicit [26]. In a Lagrangian method, the nodes of the finite element mesh are attached to the

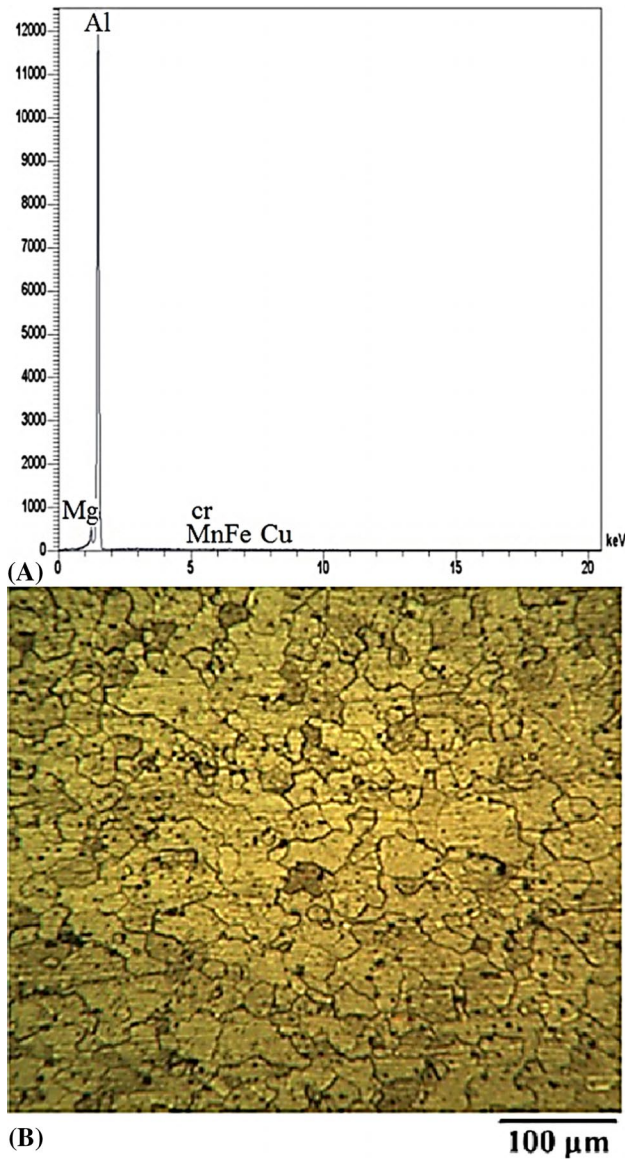


Fig. 2 a The analysis of energy dispersive spectrometry (EDS), and b the microstructure of AA5083

material points, and the meshes deform with the material. Since the nodes are coincident with the material points in the Lagrangian mesh, boundary nodes remain on the boundary throughout the evaluation of the problem. In Eulerian description, the nodes of the finite element mesh are fixed in space, and material flows through the mesh. ALE description takes advantage of both the Lagrangian formulation, where nodes are forced to move with the element and Eulerian formulation where the material goes through the mesh.

Table 1 The chemical composition of the base metal (wt %)

C	Si	Mn	P	Cr	Ni	Cu	Mg	S	Al	Fe
Value	0.5	0.4	–	0.25	–	0.1	4.8	–	Bal	0.4

Table 2 Mechanical properties of the base metal

Y.S (MPa)	UTS (MPa)	Elongation (%)	E (GPa)	Hardness (HV)
184	307	15	71	94

Table 3 Welding parameters used in this study

Sample no	Rotational speed (rpm)	Dwell time (s)	Plunge depth (mm)	Vibration frequency (Hz)
1	1500	5	2.5	17.32
2	1500	10	2.5	17.32

That maintains a high-quality mesh throughout the analysis. The three-dimensional view of the finite element analysis of FSSW process is shown in Fig. 4.

Due to the high strain rate, adiabatic heating was assumed with an inelastic heat fraction of 0.9. This term characterizes the fraction of plastic work converted into heat which is usually considered to be a constant although it can be strongly dependent on strain and strain rate. The Johnson–Cook model widely used in the ballistic and impact testing community; therefore, it is also used extensively in FE simulations of slower processes like FSW and FSSW. The Johnson–Cook equations described as:

$$\sigma = (A + B\epsilon^n)(1 + C \ln \dot{\epsilon}_p)(1 - T^{*m}) \tag{1}$$

where ϵ is equivalent plastic strain $\dot{\epsilon}_p$ is plastic strain rate for $\dot{\epsilon}_0 = 1s^{-1}$, A, B, C, m and n are the material constants. And also:

$$T^m = \frac{T - T_{room}}{T_{melt} - T_{room}} \tag{2}$$

where T is absolute temperature for $0 \leq T^* \leq 1$ and A, B, C, n, m are constant. The constants, in (Eq. 1), are obtained from simple mechanical tests such as isothermal tension or torsion tests. Table 4 shows the required constants for materials used in this work [27].

2.3 Thermal Analysis

In this analysis, the thermal response during FSSW is governed by the following equation [28, 29]:

$$\rho c_p \frac{\partial T}{\partial t} = \frac{\partial}{\partial x} \left[k_x \frac{\partial T}{\partial x} \right] + \frac{\partial}{\partial y} \left[k_y \frac{\partial T}{\partial y} \right] + \frac{\partial}{\partial z} \left[k_z \frac{\partial T}{\partial z} \right] + Q \tag{3}$$

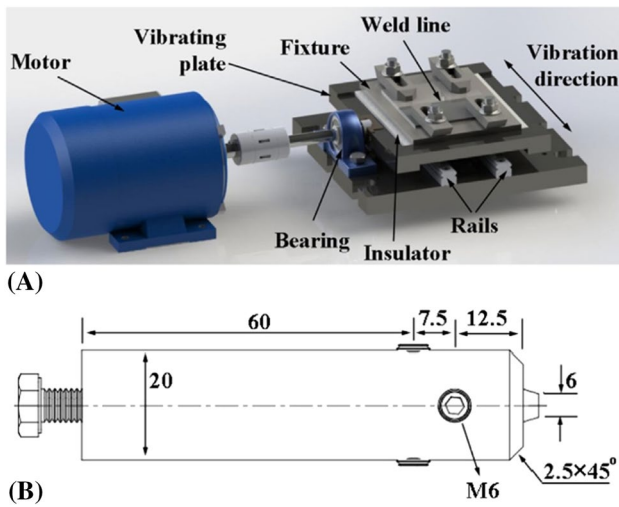


Fig. 3 a Schematic design of fixture and the set used for vibration and b geometry of pin and shoulder used for FSSW and FSSVW processes (all dimensions are in mm)

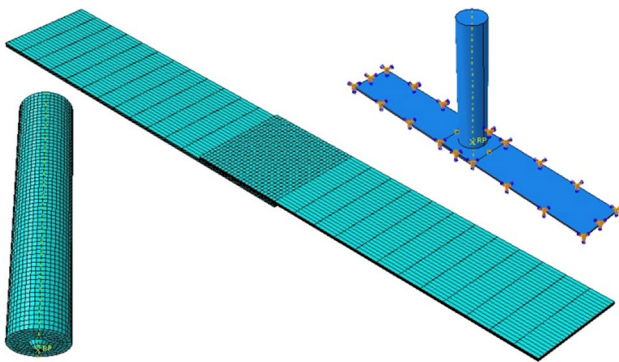


Fig. 4 The FE-mesh used for simulation of FSSW process and boundary condition

where ρ is the material density, c_p is the material specific heat, k is heat conductivity (i.e., k_x , k_y , and k_z are the heat conductivity in x , y , and z directions), T is the temperature, t is the time, and Q is the heat generation. In finite element formulation, Eq. (3) can express as:

$$C(t)\dot{T} + K(t)T = Q(t) \tag{4}$$

where, $C(t)$ is the time-dependent capacitance matrix, T is the nodal temperature vector, $K(t)$ is the time-dependent conductivity matrix, \dot{T} is the derivative of the temperature

with respect to time (i.e., dT/dt), T is the nodal temperature vector, and $Q(t)$ is the time-dependent heat vector.

The nodal temperature rate from the above equation is given by:

$$\dot{T}_i = C^{-1}(F - KT_i) \tag{5}$$

Difference integration for the nodal temperature rate gives,

$$\dot{T}_i = \frac{T_{i+1} - T_i}{\Delta t_{i+1}} \tag{6}$$

It can be expressed as:

$$T_{i+1} = (\Delta t_{i+1})\dot{T}_i + T_i \tag{7}$$

Finally, the nodal temperature rate can be written as:

$$T_{i+1} = (\Delta t_{i+1})C^{-1}(F - KT_i) + T_i \tag{8}$$

3 Results and Discussion

3.1 Microstructure

Figures 5 and 6 show the effect of vibration on microstructure and grain size for both FSSW and FSSVW processes. These results confirm that vibration during welding decreases the grain sizes of welded specimens, especially in the dwelling time of 5 s. It has been proved that the development of fine grains in the weld region in FSSW process is dependent on dislocation generation in microstructure [30, 31] and occurrence of dynamic recrystallization due to heat produced by friction [32]. In FSSVW, due to the application of vibration, more strain is applied to the material in the weld region, and strain rate enhances. Consequently, more dislocations are generated. Enhanced dynamic recrystallization leads to finer grains in the weld zone. That is a good deal with Zener–Hollomon relation [33]:

$$Z = \dot{\epsilon} \exp\left(\frac{Q}{RT}\right) \tag{9}$$

The Zener–Hollomon parameter describes the combined effect of strain rate and temperature on flow stress of metals for deformation at or below room temperature. In Eq. 9, T is the deformation temperature, Q is the activation energy, and R is the gas constant.

According to the Zener–Hollomon relation (Eq. 9), the Z parameter increases as the strain rate ($\dot{\epsilon}$) increases. The relationship between Zener–Hollomon parameter (Z) and grain size (D) is presented as [34]:

Table 4 The Johnson–Cook equation parameters for the materials used

A (MPa)	B (MPa)	n	m	Melting Temp (°K)	Transition Temp (°K)	Strain rate coefficient (C)	$\dot{\epsilon}_0$
167	596	0.551	1	893	298	0.001	1

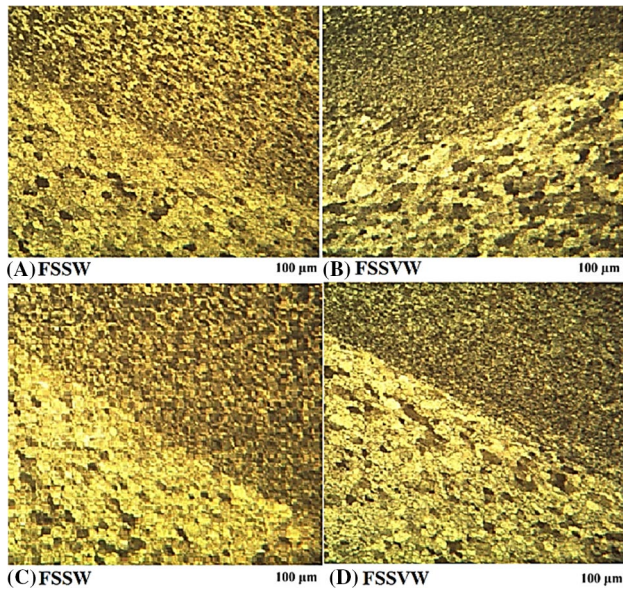


Fig. 5 Microstructure of joints developed using different welding conditions: **a** FSSW with a dwelling time of 10 s, **b** FSSVW with a dwelling time of 10, **c** FSSW with a dwelling time of 5 s, **d** FSSVW with a dwelling time of 5 s

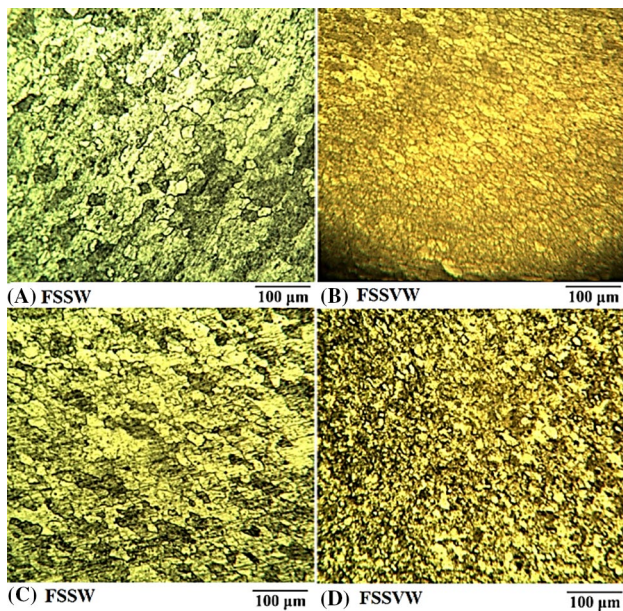


Fig. 6 Weld region microstructures of FSS-welded specimens under different conditions. **a** FSSW with a dwelling time of 10 s, **b** FSSVW with a dwelling time of 10, **c** FSSW with a dwelling time of 5 s, **d** FSSVW with a dwelling time of 5 s

$$D^{-1} = a \ln Z - b \tag{10}$$

where *a*, *b* parameters are constants. According to Eq. 9, grain size decreases, as the *Z* parameter increases.

Grain size enhancement in the dwelling time of 10 s (Fig. 5) can be related to the effect of friction heat during

welding processes. Rahmi and Abbasi [34] found that as friction between the tool and work-piece increases more heat is generated, and consequently, grains grow and grain size increase. They indicated that during FSW, grain size increased as generated heat-enhanced.

Figure 7 shows the grain size measurement data (based on Fig. 6) for different welding conditions. The results show that vibration during FSSW leads to grain size decrease of about 48% and 31% in the weld region for dwelling time of 5 and 10 s, respectively.

Fractography analysis by SEM was carried out to compare the fracture surfaces of FSS-welded and FSSV-welded specimens. Fracture surfaces are presented in Fig. 8. Both fracture surfaces show dimples which indicate ductile fracture for both samples. It has been known that in the ductile fracture, extensive plastic deformation takes place before fracture and the fundamental step before the fracture is void formation, void coalescence, and crack propagation [35]. Dimple constitution is dependent on the development of locks among dislocations, and each dimple corresponds to the void. During FSSVW, due to enhanced deformation of the material, more dislocations are generated and more locks developed among them. It leads to higher and smaller voids for FSSV-welded specimen in comparison to FSS-welded specimen (Fig. 8).

3.2 Thermal Analysis

Macrostructure and thermal simulation of samples in both FSSW and FSSVW conditions are presented in Fig. 9. Defect-free sections are visible. It is also observed in Fig. 9 that processing zones of FSV welded specimens are larger than those of FS welded specimens. That is related to the

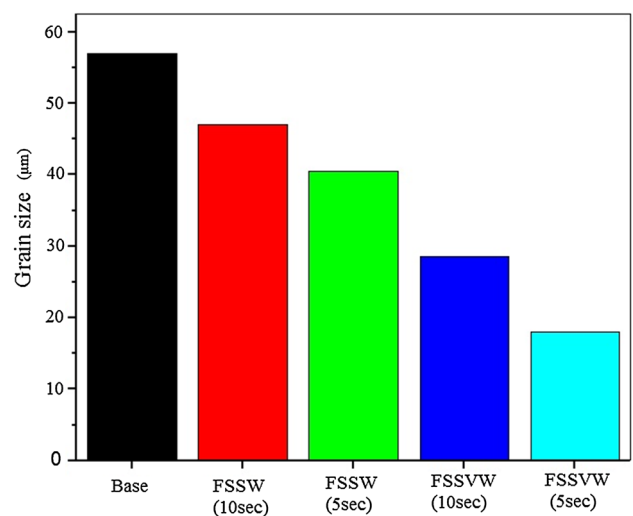


Fig. 7 Weld region grain size data for different specimens welded using different welding conditions (°C)

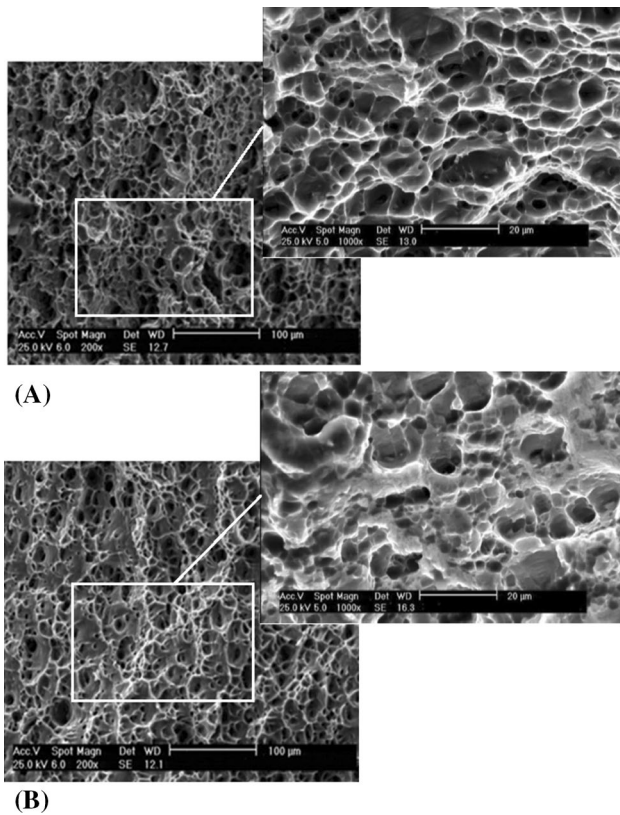


Fig. 8 SEM fracture surface of **a** FSSV-welded sample and **b** FSS-welded sample

vibrating motion of the sample during FSSVW which leads to larger processing zone. Figure 9 also shows that temperature for FSSV-welded specimen is higher than that for FSS-welded specimen.

FEM results in temperature distribution for both FSSW and FSSVW conditions, at the same step and increment time, are observed in Fig. 10. Figure 10 shows that the vibration can increase the thermal affected zone of the welding area, and also the maximum temperature obtained using vibration is higher than that obtained using FSSW.

Layouts of K-type thermocouples applied within the work-piece to measure the temperature distribution during FSSW and FSSVW processes is presented in Fig. 11. The thermocouples located under the pin at one side.

Figure 12 represents temperature histories for the studied points obtained using simulation and thermocouples. It is evident that there is good compatibility between experimental and simulated results. In all measurements, FEM results show higher temperature compared to laboratory results which it may refer to simulation conditions such as friction condition, boundary condition and also mesh sizing, etc.

Figure 12 shows that temperature results for point 1 (Fig. 11) is slightly higher than position 2 and for point 3 is higher than point 4. It can be related to the position of

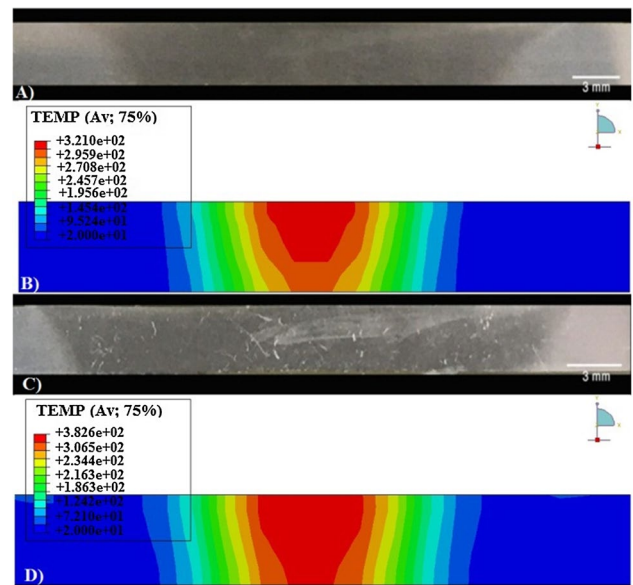


Fig. 9 Macrostructure and thermal view of **a, b** FSSW-welded and **c, d** FSSV-welded specimens

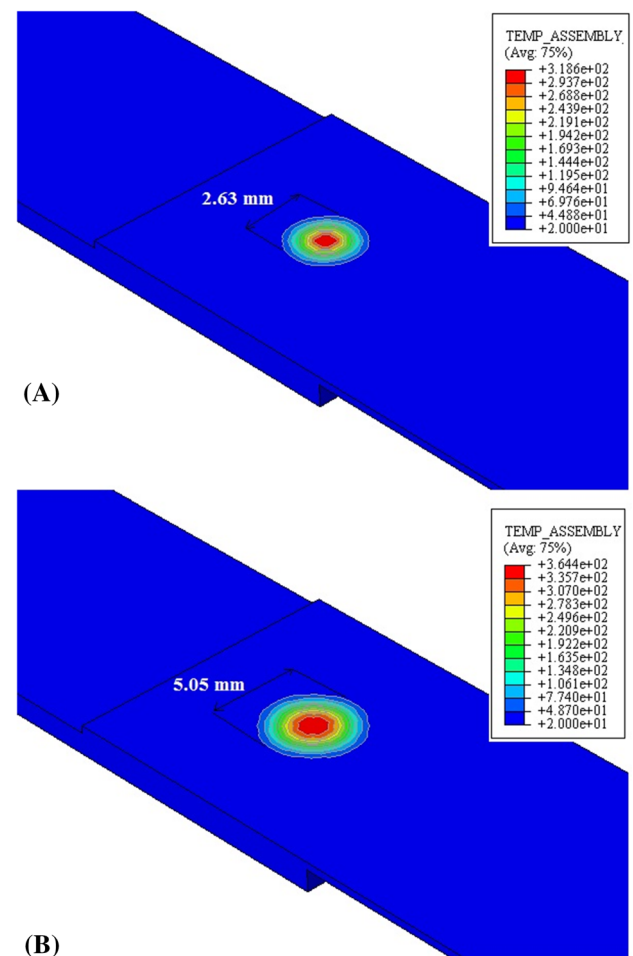


Fig. 10 Temperature distribution around the weld area for both **a** FSSW, and **b** FSSVW conditions

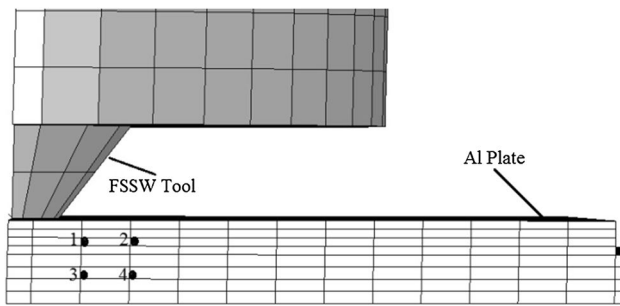


Fig. 11 Layouts of the thermocouples embedded in the workpiece to measure the temperature

these points. Points 1 and 3, comparing points to 2 and 4, are in lower distance to the tool, so higher temperatures for these points are expected. It is also observed that temperature results for points 3 and 4 are higher than points 1 and 2, respectively. Points 1 and 2 are near to surface, and due to convection, more heat is transferred to air, and correspondingly, lower temperatures are obtained.

Finally, Eq. (11) shows the general relationship between the maximum temperature T ($^{\circ}\text{C}$) and FSW parameter (ω , v) [36]:

$$\frac{T}{T_m} = K \left(\frac{\omega^2}{v \times 10^4} \right)^\alpha \tag{11}$$

where the exponent α ranges from 0.04 to 0.06, the constant K is between 0.65 and 0.75, and T_m ($^{\circ}\text{C}$) is the melting point of the alloy, ω is rotation rate (rpm), and v is traverse speed (rpm). According to Eq. (11), the maximum temperature observed should be between 0.6 and 0.9 T_m , which is in agreement with the results shown in Fig. 12.

Maximum temperature magnitudes for different specimens, relating to Fig. 12, are presented in Table 5. Based on Table 5, the maximum values of FSSV-welded specimens are higher than those welded without vibration.

4 Conclusions

In this work, the effect of workpiece vibration during FSSW in joining Al5083 specimens was investigated experimentally and numerically. The microstructure and thermal conditions were analyzed, and the results showed that weld region grain size in FSSVW process, due to more work hardening of material in the weld region, decreased compared to that in FSSW. Johnson–Cook Plasticity (JCP) theory was used to model the welding processes. There was a good agreement between experimental and FEM results about temperature distribution and presence of vibration increased the

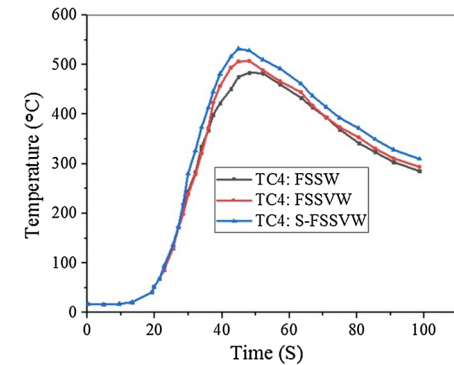
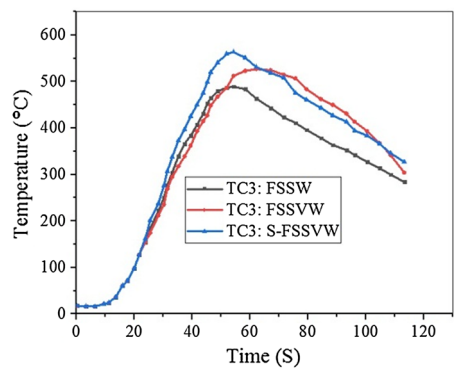
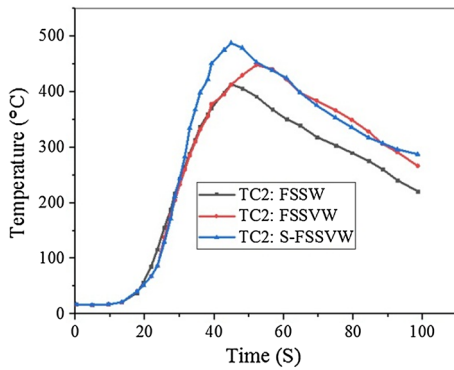
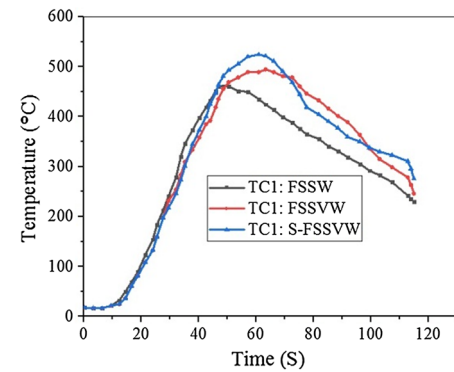


Fig. 12 Comparison among temperature histories of different points (corresponding to the layout of thermocouples presented in Fig. 11) obtained through simulation and experiment (Simulation results are denoted by S-FSSVW)

Table 5 The maximum temperature values for FSS, FSSV and S-FSSV-welded specimens obtained from results presented in Fig. 11

	TC1 (°C)	TC2 (°C)	TC3 (°C)	TC4 (°C)
FSSW	462	421	489	458
FSSVW	509	448	533	508
S-FSSVW	547	491	567	531

temperature slightly. Finally, it was concluded that FSSVW is a proper alternative process for FSSW process.

References

- Mishra, R. S., & Ma, Z. Y. (2005). Friction stir welding and processing. *Materials Science and Engineering R*, 50(1–2), 1–78.
- Nandan, R., DebRoy, T., & Bhadeshia, H. (2008). Recent advances in friction stir welding process, weldment structure and properties. *Progress in Materials Science*, 53, 980–1023.
- Lee, C. Y., Choi, D. H., Yeon, Y. M., & Jung, S. B. (2009). Dissimilar friction stir spot welding of low carbon steel and AlMg alloy by formation of IMCs. *Science and Technology of Welding and Joining*, 14(3), 216–220.
- Coelho, R. S., Kostka, A., Sheikhi, S., Dos Santos, J., & Pyzalla, A. R. (2009). Microstructure and mechanical properties of an AA6181-T4 aluminium alloy to HC340LA high strength steel friction stir overlap weld. *Advanced Engineering Materials*, 10(10), 961–972.
- Coelho, R. S., Kostka, A., Dos Santos, J., & Pyzalla, A. R. (2009). EBSD technique visualization of material flow in aluminum to steel friction-stir dissimilar welding. *Advanced Engineering Materials*, 10(12), 1127–1133.
- Cavaliere, P., Cerri, E., Marzoli, L., & Dos Santos, J. (2004). Friction stir welding of ceramic particle reinforced aluminium based metal matrix composites. *Applied Composite Materials*, 11(4), 247–258.
- Wert, J. A. (2003). Microstructures of friction stir weld joints between an aluminum-base metal matrix composite and a monolithic aluminum alloy. *Scripta Materialia*, 49(6), 607–612.
- Mishra, R. S., & Mahoney, M. W. (2007). *Friction stir welding and processing*. Ohio: ASM International.
- Uejii, R., Fujii, H., Cui, L., Nishioka, A., Kunishige, K., & Nogi, K. (2006). Friction stir welding of ultrafine grained plain low carbon steel formed by the martensite process. *Materials Science and Engineering A*, 423(1–2), 324–330.
- Fujii, H., Cui, L., Maeda, M., & Nogi, K. (2006). Effect of tool shape on mechanical properties and microstructure of friction stir welded aluminum alloys. *Materials Science and Engineering A*, 419(1–2), 25–31.
- Fujii, H., Cui, L., Tsuji, N., Maeda, M., Nakata, K., & Nogi, K. (2006). Friction stir welding of carbon steels. *Materials Science and Engineering A*, 429(1–2), 50–57.
- Al-Shahrani, A., & Wynne, B. P. (2010). Effect of dwell time on friction stir spot welded dual phase steel. *Advanced Materials Research*, 83, 1143–1150.
- Su, P., Gerlich, A., North, T. H., & Bendzsak, G. J. (2007). Inter-mixing in dissimilar friction stir spot welds. *Metallurgical and Materials Transactions A*, 38(3), 584–595.
- Guerra, M., Schmidt, C., McClure, J. C., Murr, L. E., & Nunes, A. C. (2002). Flow patterns during friction stir welding. *Materials Characterization*, 49(2), 95–101.
- Yang, Q., Mironov, S., Sato, Y. S., & Okamoto, K. (2010). Material flow during friction stir spot welding. *Materials Science and Engineering A*, 527(16–17), 4389–4398.
- Tuncel, O., Aydin, H., Tutar, M., & Bayram, A. (2016). Mechanical performance of friction stir spot welded AA6082-T6 sheets. *International Journal of Mechanical and Production Engineering*, 4(1), 114–118.
- Dey, A., Saha, S. C., & Pandey, K. M. (2014). Study of mechanical properties change during friction stir spot welding of aluminum alloys. *Current Trends in Technology & Sciences*, 3(1), 26–33.
- Baek, S. W., Choi, D. H., Lee, S. Y., Ahn, B. W., Yeon, Y. M., Song, K., et al. (2010). Microstructure and mechanical properties of friction stir spot welded galvanized steel. *Materials Transactions*, 51(5), 1044–1050.
- Sheikhhasani, H., Sabet, H., & Abasi, M. (2016). Investigation of the effect of friction stir spot welding of BH galvanized steel plates on process parameters and weld mechanical properties. *Engineering Technology & Applied Science Research*, 6(5), 1149–1154.
- Kulekci, M. K. (2014). Effects of process parameters on tensile shear strength of friction stir spot welded aluminium alloy (EN AW 5005). *Archives of Metallurgy and Materials*, 59(1), 221–224.
- Jweeg, M., Tolephih, M., Muhammed, M., & Sadiq, G. (2016). Numerical and experimental analysis of transient temperature and residual thermal stresses in friction stir welding of aluminum alloy 7020-T53. *ARPN Journal of Engineering and Applied Sciences*, 11(19), 143–152.
- Khuder, A. W. H., Muhammed, M. A., & Ibrahim, H. K. (2017). Numerical and experimental study of temperature distribution in friction stir spot welding of AA2024-T3 Aluminum Alloy. *Journal of Innovative Research in Science, Engineering and Technology*, 6(5), 7281–7291.
- Quazi, I. A., Shete, M. T., & Quazi, M. A. (2015). Thermo-mechanical characterization of friction stir spot welded HDPE sheets. *Journal for Science Research and Development*, 3(4), 746–769.
- Campanelli, L. C., Antonialli, A. I. S., de Alcântara, N. G., Bolfarini, C., Suhuddin, U. F. H., & dos Santos, J. F. (2013). Lap shear test of a magnesium friction spot joint: numerical modeling. *Tecnologia em Metalurgia, Materiais e Mineração*, 10(2), 97–102.
- ASTM-E112-13. (2013). *Standard test methods for determining average grain size*. West Con shohocken: ASTM International.
- ABAQUS/6.14.2. (2016). Providence, RI, USA: Dassault Systems Simulia Corp.
- Yalavarthy, H. (2009). Friction stir welding process and material microstructure evolution modeling in 2000 and 5000 series of aluminum alloys. All Thesis, Clemson University.
- Getting Started with Abaqus/Explicit: Hibbit, Karlsson & Sorensen, Inc., version 6.14 (2004).
- Belytschko, T., Liu, W., & Moran, B. (2000). *Nonlinear finite elements for continua and structures*. Hoboken: Wiley.
- Woo, W., Ungar, T., Feng, Z., Kenik, E., & Clausen, B. (2010). X-ray and neutron diffraction measurements of dislocation density and subgrain size in a friction-stir-welded aluminum alloy. *Metallurgical and Materials Transactions A*, 41, 1210–1216.
- Abbasi, M., Abdollahzadeh, A., Omidvar, H., & Bagheri, B. (2016). Rezaei M (2016) Incorporation of SiC particles in FS welded zone of AZ31 Mg alloy to improve the mechanical properties and corrosion resistance. *International Journal of Materials Research*. <https://doi.org/10.3139/146.111369>.
- Etter, A. L., Baudin, T., Fredj, N., & Penelle, R. (2007). Recrystallization mechanisms in 5251-H14 and 5251-O aluminum friction stir welds. *Materials Science and Engineering A*, 445–446, 94–99.
- Callister, W. D. (2007). *Materials science and engineering: an introduction*. Hoboken: Wiley.

34. Rahmi, M., & Abbasi, M. (2017). Friction stir vibration welding process: modified version of friction stir welding process. *International Journal of Advanced Manufacturing Technology*, *90*, 141–151.
35. Kalaki, A., Ketabchi, M., & Abbasi, M. (2014). The joining of D2 and M2 tool steels: analysis of microstructure and mechanical properties. *International Journal of Materials Research*, *105*, 764–769.
36. Arbegast, W.J. & Hartley, P.J. (1998). Friction stir weld technology development at Lockheed Martin Michoud space systems—An overview. *Proceedings of the Fifth In Con on Trends in Weld Research* (pp. 541–554). Pine Mountain, GA, USA.

Publisher's Note Springer Nature remains neutral with regard to jurisdictional claims in published maps and institutional affiliations.



Behrouz Bagheri took his master degree in Materials Science and Engineering from Amirkabir University of Technology. Now, he works in Amirkabir University as a researcher.



Mahmoud Abbasi is now faculty member of University of Kashan. He has a Ph.D. degree in Materials Science and Engineering from Amirkabir University of Technology.



Mohammad Givi now works in University of Kashan as a researcher. He received his master degree in Materials Science and Engineering from University of Kashan.